J. Phys. B: At. Mol. Phys. **20** (1987) 2899-2910. Printed in the UK

Electron–helium and electron–neon scattering cross sections at low electron energies using a photoelectron source

Vijay Kumar†, E Krishnakumar‡ and K P Subramanian†

† Physical Research Laboratory, Navrangapura, Ahmedabad-380009, India
‡ Jet Propulsion Laboratory, Pasadena, CA, USA

Received 9 July 1986, in final form 25 November 1986

Abstract. Absolute electron-helium and electron-neon scattering cross sections have been measured at low electron energies using the powerful technique of photoelectron spectroscopy. The measurements have been carried out at 17 electron energies varying from 0.7 to 10 eV with an accuracy of ±2.7%. The results obtained in the present work have been compared with other recent measurements and calculations.

1. Introduction

The study of electron-atom and electron-molecule scattering at low energies is important for the understanding of weakly ionised plasmas as well as weakly populated neutral clouds of excited species. The best examples of where both these processes dominate are gas discharges, ionospheres of different planets, interstellar clouds etc. The scattering processes at low electron energies are difficult to understand as neither theoretical nor experimental work can be carried out easily at these energies. In theory, better approximations of the interaction potentials are required, taking into account both static and dynamic Coulomb interactions and spin exchange with atomic electrons. Experimentally, in scattering problems the low electron energy region becomes more and more challenging and requires sophisticated modern techniques to obtain more accurate data. A direct comparison of theory could conveniently be made with total scattering cross section measurements at low electron energies.

In recent years, the electron scattering cross section measurements for helium and neon have been carried out by a large number of research groups. The latest measurements in the case of electron-helium scattering have been made by Stein *et al* (1978) and Nickel *et al* (1985) using transmission techniques at electron energies ranging from 0.25 to 24 eV and 4 to 300 eV respectively. Using the time of flight technique, Kennerly and Bonham (1978) and Charlton *et al* (1980) measured the total electron-helium scattering cross sections at electron energies from 0.5 to 50 eV and 2 to 50 eV respectively. The most precise theoretical calculations in this electron energy region have been reported by Nesbet (1979) using variational approximations to express the helium ground-state wavefunction. A direct comparison shows that the measured values given by Stein *et al* (1978) compare very well with the values reported by Nesbet (1979) at electron energies higher than 4.5 eV, but below this energy their values are less than those reported by Nesbet. A similar picture has also emerged for cross

0022-3700/87/122899+12$02.50

sections reported by Kennerly and Bonham (1978) at energies higher than 2.5 eV, but at lower energies their cross sections are higher.

Electron-neon scattering cross section measurements at low electron energies have been carried out by Salop and Nakano (1970) at electron energies between 0.37 and 20 eV using a modified Ramsauer technique. This was followed by measurements by Stein *et al* (1978) between 0.25 and 24 eV, Nickel *et al* (1985) between 4 and 300 eV, both of whom used transmission techniques, and O'Malley and Crompton (1980) between 0 and 2.3 eV using a swarm technique. Most of these measurements compare very favourably with the latest theoretical values for cross sections reported by McEachran and Stauffer (1985). However, there is still a case for making more measurements at electron energies lower than about 2 or 3 eV.

In the light of the above arguments, it is clear that more measurements in this direction are needed, possibly using new techniques. In the present experiment, absolute e-He and e-Ne scattering cross sections at low electron energies from 0.7 to 10 eV have been measured using the powerful technique of photoelectron spectroscopy. It has previously been demonstrated by Kumar and Krishnakumar (1981b) that the technique of photoelectron spectroscopy could be used to measure electron-atom and electron-molecule scattering cross sections at low electron energies. Since the experimental set-up (Kumar and Krishnakumar 1981b) was not specifically built for electron scattering studies, it had a few limitations. In the first place, the scattering in the accelerating and analysing regions in the photoelectron spectrometer could not be eliminated completely and, secondly, only relative values of the scattering cross sections could be obtained. In view of this, a new experimental set-up has been designed and constructed which takes care of all these limitations.

2. Experimental set-up

Electrons are produced by photoionisation of a source gas in a small ionisation region, which in most set-ups is located close to the electron energy analyser. In the present experiment, noble gases like argon, krypton and xenon were used as the source gas. When VUV photons from strong atomic emission lines are allowed to impinge on the source gas, the gas is photoionised and electrons of two energies are emitted corresponding to the $^2P_{1/2}$ and $^2P_{3/2}$ states of the ion thus produced. With photons corresponding to a single wavelength and using one source gas at a time, two electron energies would be accessible. With the various combinations of photons corresponding to three wavelengths (58.4, 73.6 and 74.4 nm) and argon, krypton and xenon as source gases, 18 electron energies are accessible from 0.7 to 10 eV. Two of the electron energies are very close to each other and cannot be resolved, with the result that, for all practical purposes, only 17 electron energies are available for carrying out the scattering experiment.

The resonant emission lines He I (58.4 nm) and Ne I (73.6 and 74.4 nm) are produced by microwave discharge of helium and neon gas respectively. These resonant lines are monochromatic; the energy spread of these lines depends upon the pressure of the helium or neon gas used. The pressure of the emitting gas in the discharge tube is kept constant throughout the experiment. For this purpose a microwave generator (Ophthos Instrument Co., MD) and an Evanson cavity were used at 2450 MHz with an average microwave power of 100 W. The monochromatic VUV photons thus produced interact with the source gas in the ionisation region, generating photoelectrons

at two discrete energies. The intensity of the photon beam is monitored using a beam splitter, which can be isolated from the light source using a gate valve. The residual gas in the light source is rapidly removed by differentially pumping the region between the gate valve and the light source by a combination of a root pump and a mechanical pump. The beam splitter consists of a high transparency wire mesh mounted at an angle of 45° to the beam axis. More than 90% of the light is transmitted and the rest is reflected towards a light detector, which consists of a perspex light pipe frosted from the sides and an EMI 6199 photomultiplier with a S-11 spectral response. The receiving end of the light pipe is coated with a scintillator, p-terphenyl, to convert VUV into visible light. Any change in the light intensity could thus be monitored using the beam splitter and the change in intensity, if any, during the experiment could be incorporated in the results. This beam splitter monitored light emission of all wavelengths corresponding to the resonance lines of helium or neon in the VUV region along with the other visible lines which cannot energetically photoionise any gas. It was found that the change in total intensity observed by the beam splitter did not have a one to one correspondence to the change in the VUV line intensity. To avoid the visible emission reflected by the wire mesh from entering the light pipe, an unbacked thin-film metal filter of aluminium with a thickness of about 1500 Å was provided in front of the receiving end of the light pipe. The aluminium thin film transmits light in the VUV region only, from about 170 to 800 Å (Samson 1967). The complete beam splitter system was enclosed in a stainless steel chamber and evacuated by a diffstak pump (Edwards MK2 160/700P) at a rate of 700 l s^{-1} and backed by a rotary pump (Edwards EDM 20A).

The VUV photon beam thus produced was allowed to pass through a large number of circular baffles before emerging into a small region where photoionisation of the source gas takes place. The pressure of the source gas is kept low (less than 10^{-3} Torr) to avoid any electron scattering by the source gas atoms. The photoelectrons thus produced were energetically analysed using a cylindrical mirror analyser and were detected by a channeltron (Mullard B419BL) operated in the counting mode. After proper amplification, the signals were stored in a home-made microprocessor-controlled multichannel analyser operated in the time mode. The ionisation region, the accelerating region, the analysing region of the cylindrical mirror analyser and the channeltron region were all differentially pumped by a very fast diffstak pump (Edwards MK2 250/2000P) at a rate of 2000 l s^{-1} and by a mechanical pump at a corresponding rate (Edwards E2M40).

The cylindrical mirror analyser had a slit to slit focusing geometry and was essentially similar to the one designed by Gardner and Samson (1973). The photoelectrons produced in the ionisation region were allowed to enter the first slit of the analyser at an angle of 54° 44′ ± 3°. The diameters of the inner and outer cylinders were 4 and 10 in respectively, while the distance between the two slits (centre to centre) was kept at 6.264 in, in accordance with the best focusing conditions around 55°. A slit width of 2 mm was used for both the slits. The electron detector, the channeltron, was always kept at a pressure less than 10^{-4} Torr.

The photoelectrons produced in the small photoionising region by the interaction of VUV photons of discrete energy with the source gas at low pressure are allowed to be scattered by the target gas. The scattering path length is limited between the centre and the slit of the ionising region over the 2π geometry. Without any target gas the amplitudes of the photoelectron peaks produced by the source gas were monitored at a fixed but low source gas pressure in the ionisation region. The target gas was then

introduced at a series of different pressures and the extent of the decrease in the amplitude of the photoelectron peak was noted. This decrease is attributed to electron scattering by target gas species whose number density increases with increasing pressure.

With neither source nor target gas present in the ionisation region, the background pressure in the whole system is 10^{-6} Torr. With the source gas introduced at a fixed pressure in the photoionisation region, the pressures in the analysing region and the beam splitter chamber were found to be 8×10^{-6} and 10^{-4} Torr respectively. With a maximum pressure of about 0.025 Torr in the scattering region, the pressures in the analysing region and the beam splitter chamber were found to be 8.2×10^{-5} and 10^{-3} Torr respectively. The vacuum in the channeltron region was always found to be better than 10^{-4} Torr; around 6×10^{-5} Torr under the worst conditions. The absolute gas pressure was measured using an MKS Baratron capacitance manometer (head 310 MH-1).

A provision had been made to continuously bake the cylindrical mirror analyser at a constant temperature of 80 °C for a few days. An arrangement had also been made to have a high pressure RF discharge of argon near the scattering region. Both these methods ensured proper cleanliness of all the slits, with the result that practically no effects due to contact potentials could be observed. They also prevented the possible lens effects from occurring; these effects occur due to different contact potentials between the two slits of the accelerating region. As a result the photoelectron peaks appeared at the calculated energies and the value of the CMA constant did not change during the course of the experiment for a particular set of electron energies. It may however be stressed that in the present experiment the scattering of electrons takes place first and then the energy analysis of the electrons is carried out using a CMA, which does not have the problem of contact potential present in the system.

The collection efficiency of the CMA has been previously reported as a function of electron energy (Kumar and Krishnakumar 1981a). However, it may be noted that the measurement of the scattering cross section is independent of the collection efficiency of the CMA. At a particular electron energy, the amplitude of the photoelectron peak is monitored with initially no target gas in the scattering region and then as a function of the target gas pressure. As a result the scattering cross section at this particular energy is measured. A similar procedure is adopted for cross section measurements at other electron energies.

3. Method

A method has been formulated in order to obtain the total absolute cross section for electron scattering at low energies. The method followed is different, when the source and target atoms are the same, from that used when the source and target atoms are different. In the present experiment the source atoms used for producing photoelectrons were argon, krypton and xenon while the target atoms involved in the scattering cross section measurements were helium and neon. The method followed when the source and target atoms are different is described below.

When a beam of electrons is passing through a scattering medium, the transmitted intensity is given by

$$I_e = I_{e0}\exp(-n\sigma x)$$

where I_{e0} is the initial intensity of the electrons, n is the number density of the target

atoms, x is the scattering path length and σ is the total electron target scattering cross section at a particular energy. In the experiment, I_{e0} and I_e are the amplitudes of the photoelectron peaks of a single electron energy before and after the electron scattering respectively.

The pressures of the source gas inside and outside the ionisation region are P' and p', respectively, which remained constant throughout the experiment. At two pressures P_1 and P_2 of the target gas, the amplitudes of the photoelectron peak are given by

$$I_{e1} = I_{e01} \exp[-(P' + P_1)n_0\sigma x/760]$$
$$I_{e2} = I_{e02} \exp[-(P' + P_2)n_0\sigma x/760]$$

where n_0 is Loschmidt's number. The ratio of the observed peak amplitudes at the two different pressures is given by

$$I_{e1}/I_{e2} = (I_{e01}/I_{e02}) \exp[-(P_1 - P_2)n_0\sigma x/760]. \tag{1}$$

The electrons produced in the small photoionisation region relate to the average photon intensity $\langle I_\lambda \rangle$ and the pressure:

$$\frac{I_{e01}}{I_{e02}} = P'\langle I_\lambda \rangle_1 / P'\langle I_\lambda \rangle_2 = \langle I_\lambda \rangle_1 / \langle I_\lambda \rangle_2$$
$$= (I_{\lambda 01}/I_{\lambda 02}) \exp[-(k/760)(P_1 - P_2)(al_1 + l_2)] \tag{2}$$

where k and k' are the photoabsorption coefficients of the target and source gases respectively at a particular wavelength. k' is eliminated in ratio (2) I_{e01} and I_{e02}. $I_{\lambda 01}$ and $I_{\lambda 02}$ are the incident photon intensities at pressures P_1 and P_2. The factor a is the ratio of pressures p and P, which have been defined earlier. The pressure measurements of P and p over a range from 0.025 to 10^{-3} Torr indicated that the factor a was constant throughout this pressure range. The lengths l_1 and l_2 are as shown in figure 1. The value of a was found to be 0.124 while the lengths l_1 and l_2 and x from the geometry of the apparatus were 30, 2.58 and 2.37 cm respectively. l_2 and x were derived geometrically taking into account the average length of the effective ionisation region along the direction of the photon beam.

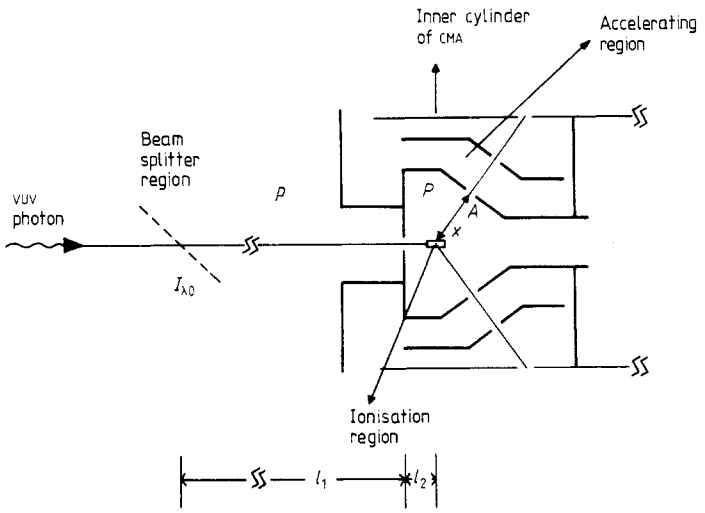

Figure 1. Schematic diagram showing the ionisation and electron scattering regions in the cylindrical mirror analyser of the photoelectron spectrometer.

Substituting equation (2) into equation (1) and simplifying, one obtains

$$\ln(I_{e2}I_{\lambda 01}/I_{e1}I_{\lambda 02}) = (P_1 - P_2/760)[n_0\sigma x + k(al_1 + l_2)] \quad (3)$$

for which $I_{\lambda 01}$ and $I_{\lambda 02}$ could be determined from the beam splitter. At the incident photon wavelengths of the resonant lines used (He I and Ne I lines at 58.4, 73.6 and 74.4 nm), the photoabsorption coefficient is negligibly small. Therefore the expression $k(al_1 + l_2)$ in equation (3) could be safely neglected. However, this would not be true for incident photon wavelengths of higher energies, where the photoabsorption coefficient would be appreciable. From equation (3), knowing all other parameters and constant factors, the total electron scattering cross sections σ for helium and neon could be calculated as a function of electron energy.

4. Error analysis

The errors in the experiments that measure total electron-atom scattering cross sections, can conveniently be classed as follows: multiplicative, such as errors in pressure, temperature or scattering path length; additive, such as errors because of counting statistics; and cross section shape errors caused by the forward scattering of electrons, gas impurities and uncertainty in the incident electron energy. The complete description of all these contributing errors is given below in order to determine an estimate of the upper limit of the actual error. The most probable estimate of the accuracy of the experiment is also given below.

4.1. Pressure measurement and instrument calibration

The gas pressure was read by means of an MKS Baratron capacitance manometer (model 310 BH-1). This manometer was capable of measuring pressures up to a maximum of 1 Torr. In the experiment the source gas was introduced at a fixed pressure of 10^{-3} Torr and the target gas pressure was varied up to 0.025 Torr. The systematic errors given by the manufacturer at these two extreme pressures were ±0.15 and ±0.09% respectively. The larger systematic error of ±0.15% is considered in calculating the most probable estimate of accuracy of the experiment.

I_{e1} was always found to be linear with respect to source gas pressure at constant I_λ. The target gas pressure was varied to a maximum value of 0.025 Torr. However this pressure was achieved only rarely. The mean free path at this pressure is less than x, so there is a chance that multiple scattering of electrons takes place. If multiple scattering is predominant, the graph between $\ln[(I_{e2}I_{\lambda 01})/(I_{e1}I_{\lambda 01})]$ and the target gas pressure would tend to deviate from a straight line at high pressures. In figure 2 no deviation from a straight line at pressures around 0.025 Torr can be seen. It is therefore obvious that multiple scattering is mainly ineffective at pressures up to 0.025 Torr.

The target gas is directly introduced into the ionisation/scattering region by means of combining a 6 in long stainless steel bellow (0.5 in ID) and a 12 cm long stainless steel tube (8 mm ID). The pressure is measured by an MKS Baratron capacitance manometer using similar combinations of bellow and tube. In both cases the tubes terminate very close to the ionisation/scattering region. The gas flow is continuous due to vigorous differential pumping through the various apertures (slits) around the target. Initially the pressure of the target gas may not be uniform, but the pressure equilibrium is quickly established. This happens when the combined conductance of the gas introducing lines as well as pressure measuring lines in the present experiment

is slightly greater (ratio 2.3 : 1.7) than the conductance of the apertures in the scattering region. Therefore pressure drops in the system would be negligibly small.

4.2. Reference pressure

The reference pressure end of the capacitance manometer was evacuated to a pressure of less than 10^{-5} Torr. Errors introduced because of this reference pressure would be negligible.

4.3. Thermal transpiration

The temperature of the capacitance manometer sensor head was maintained at 318 K, while the temperature of the scattering region where the pressure was measured was 300 K. Thus we might expect the pressure in the scattering region to be slightly less than the pressure indicated by the MKS unit head, due to thermal transpiration effects. The effects of thermal transpiration have been calculated in the present work along the lines suggested by Edmonds and Hobson (1965). It is found that using thermostatted MKS readings, the value of pressure in the scattering chamber has to be raised by 2.9%. This pressure correction has been made in all of our measurements and scattering cross sections have been calculated accordingly. The only other error which occurred was due to inaccuracy in the measurement of temperature. This could be as high as ±1 °C, which would introduce a maximum error of ±0.4%.

4.4. Scattering in the accelerating region

The electron scattering of helium and neon atoms takes place in the photoionisation/scattering region. The accelerating and analysing regions were differentially pumped. In spite of that, some electron-target scattering takes place in the accelerating region. The pressure above slit A in the accelerating region was measured by a MKS capacitance manometer. Under the worst conditions, when the target gas pressure in the ionisation region is at a maximum, i.e. 0.025 Torr, it is 0.002 Torr above the slit A and about 8.2×10^{-5} Torr above the entrance slit of the cylindrical mirror analyser. In other words there is a large differential pressure established along the accelerating region. Knowing x and the length along the accelerating region, it has been found that the errors due to scattering in this region amount to ±0.6%.

4.5. Scattering path length

The scattering path length x is the distance between the centre of the photoionisation region and the first slit of the accelerating region. The error introduced in the measurement of this length is ±2.1%. This includes the error in the scattering path length due to the extension of the photon beam along the gas column.

4.6. Counting statistics

This introduced an error of ±1.5% under the worst conditions.

4.7. Forward scattering

Forward scattering of electrons can lead to a significant reduction in the measured cross section. The electrons elastically scattered in the forward direction may undergo

a very small change in their energy. In the present experiment, the scattering of electrons takes place first and then the energy analysis is carried out. The photoelectron peaks corresponding to the $^2P_{1/2}$ and $^2P_{3/2}$ states of the source ion show a background noise level associated with these peaks. The forward scattering does not give any contribution to the photoelectron peaks but contributes close to the rising edge of the peak and the associated background level. This background level varies with the target gas pressure, helping us to find qualitatively the contribution of the electrons scattered in the forward direction. It was estimated that in the electron energy range below 10 eV the maximum error due to forward scattering was ±0.5%.

4.8. Gas impurity

The source gases argon, krypton and xenon and the target gases helium and neon were obtained from Indian Oxygen (argon only) and British Oxygen and were 99.95% pure. Argon, helium and neon were further purified by passing through a liquid nitrogen trap while krypton and xenon were passed through a trap filled with an alcohol-acetone-liquid-nitrogen slurry. It appears that the error due to the sample gas impurity could safely be considered negligible.

4.9. Uncertainty in incident electron energy

Photoelectrons are produced by the interaction of photons, from the resonant emission lines of some noble atoms, and source gases, which are also atoms. Because of this there is almost a negligible uncertainty in fixing the electron energy.

The coherent sum of all these errors acted as an estimate of the upper limit of the actual error. In the present experiment it was ±5.3%. The incoherent sum was obtained by adding the squares of all the errors and taking the square root of the total sum. The incoherent sum represented the most probable estimate of the accuracy of the experiment. In the present experiment the most probable error was estimated to be ±2.7%.

5. Results and discussion

The electron scattering cross sections for helium and neon were measured by the method given in § 3. In equation (3) all the parameters I_{e1}, I_{e2}, $I_{\lambda 01}$, $I_{\lambda 02}$, P_1 and P_2 could be determined experimentally and the cross section, σ, could be calculated. A necessary test of the present cross section measurements is provided by the frequent checks of the dependence of the ratio $(I_{e2}I_{\lambda 01})/(I_{e1}I_{\lambda 02})$ on the target gas pressure. Figure 2 shows graphs of $\ln[(I_{e2}I_{\lambda 01})/(I_{e1}I_{\lambda 02})]$ against target gas pressure for both helium and neon. In this particular case, P_1 is zero and P_2 is varying. For the sake of convenience only three electron energies for both helium and neon have been shown in the figure.

The total electron-helium scattering cross sections are shown in figure 3 for 17 electron energies ranging from 0.7 to 10 eV. The results of the present experiment are shown along with those reported by Nesbet (1979), Stein *et al* (1978), Kennerly and Bonham (1978) and Nickel *et al* (1985). Scattering cross section values as measured by Nickel *et al* (1985) have been reported only at five electron energies between 4 and 10 eV. Stein *et al* (1978) have measured the cross sections at ten electron energies

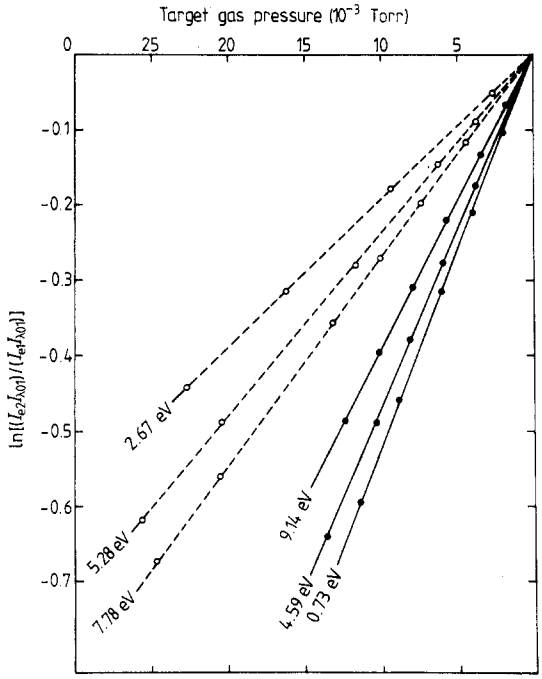

Figure 2. Plot of $\ln[(I_{e2}I_{\lambda 01})/(I_{e1}I_{\lambda 02})]$ against target gas pressure for: ——, helium; - - -, neon.

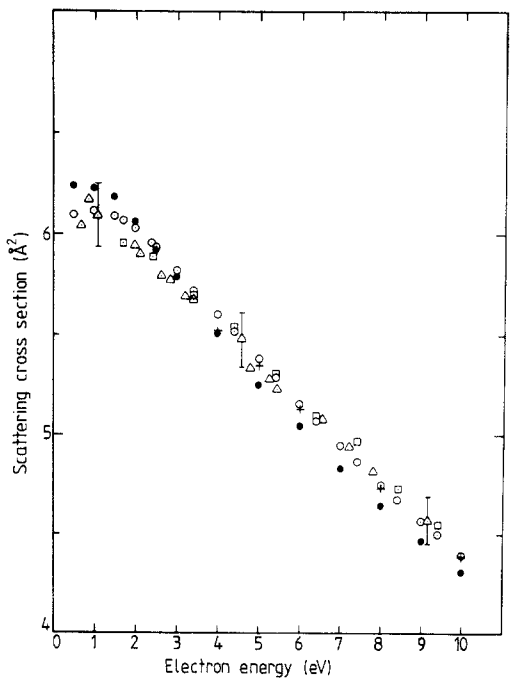

Figure 3. Total electron-helium scattering cross sections as a function of the incident electron energy from 0.7 to 10 eV obtained by various researchers: ⊙, Nesbet (1979); ⊡, Stein *et al* (1978); ●, Kennerly and Bonham (1978); +, Nickel *et al* (1985); △, present work.

ranging from 1.7 to 10.4 eV while Kennerly and Bonham have reported the data at 13 energies between 0.5 to 10 eV. Also shown in figure 3 are the results of the variational calculations of electron-helium scattering cross sections at a large number of energy points between 0.5 and 10 eV (Nesbet 1979). These calculations are accurate to within the error estimate of less than 1% and the results reported are considered to be the best known so far. The results obtained in the present work are comparable with those by Stein *et al* (1978) and also by Nickel *et al* (1985) at higher electron energies. Our values compare very well with those reported by Nesbet (1979). The measured values given by Kennerly and Bonham below 2.5 eV are higher than those reported by both the present investigators and Nesbet, while at electron energies larger than 4 eV their cross sections are smaller. The scattering cross sections as measured in the present work have been summarised in table 1 along with the results of Nesbet (1979). The percentage difference between the two cases has also been tabulated as a function of the electron energy.

Table 1. Total electron scattering cross sections. A comparison of the results obtained in the present work with those reported by Nesbet (1979).

Electron energy (eV)	Electron scattering cross sections (Å^2)		Difference %
	Present work	Nesbet (1979)	
0.73	6.04	6.105	−1.06
0.91	6.16	6.115	0.74
1.09	6.09	6.110	−0.33
2.00	5.94	6.027	−1.44
2.18	5.90	5.985	−1.42
2.67	5.79	5.890	−1.70
2.85	5.77	5.855	−1.45
3.23	5.69	5.770	−1.39
3.41	5.68	5.735	−0.96
4.59	5.48	5.465	0.27
4.77	5.33	5.430	−1.84
5.28	5.28	5.310	−0.56
5.46	5.23	5.275	−0.85
6.55	5.08	5.040	0.79
7.22	4.94	4.895	0.92
7.78	4.81	4.785	0.52
9.14	4.57	4.540	0.66

The total electron-neon scattering cross sections as measured in the present work are shown in figure 4 at 17 electron energies ranging from 0.7 to 10 eV. Also shown in the figure are cross section data reported by McEachran and Stauffer (1985), Nickel *et al* (1985), O'Malley and Crompton (1980) and Stein *et al* (1978). Cross section values measured by Nickel *et al* (1985) have been reported at only five electron energies between 4 and 10 eV. O'Malley and Crompton (1980) derived their cross sections from momentum transfer measurements and data have been reported only up to 2.3 eV. Stein *et al* (1978) have reported the cross sections for only five electron energies ranging from 2 to 10 eV. Results have been presented by McEachran and Stauffer (1985) for scattering from neon using the adiabatic-exchange approximation with the polarisation

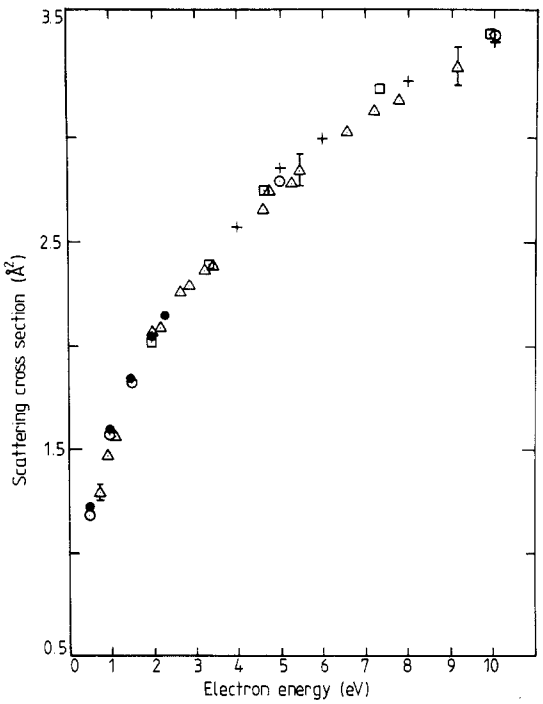

Figure 4. Total electron-neon scattering cross sections as a function of incident electron energy from 0.7 to 10 eV obtained by various researchers: ⊙, McEachran and Stauffer (1985); +, Nickel *et al* (1985); ●, O'Malley and Crompton (1980); ⊡, Stein *et al* (1978); △, present work.

potential scaled to the correct asymptotic form. Our results shown in figure 4 compare very well with those reported by other investigators, within the experimental errors discussed earlier.

6. Conclusion

From the results discussed above, it is clear that electron-helium and electron-neon scattering cross sections measured in the present experiment at electron energies from 2 to 10 eV compare very well with those reported by other investigators within the stipulated experimental errors. Below 2 eV there are not many measurements reported in the literature. In the case of electron-helium scattering, there are only two measurements reported so far; one by Kennerly and Bonham (1978) and the other reported by the authors in this paper. A similar situation also seems to prevail in the study of electron-neon scattering. The only measurement made other than in the present experiment is by O'Malley and Crompton (1980). In both these cases, i.e. where electron-helium and electron-neon scattering cross sections have been determined at electron energies less than 2 eV, our results show excellent agreement with the few other measurements that have been made. However, it appears (figure 3) that electron-helium scattering results below 1 eV, as measured in present experiment, may be more accurate than those obtained in the only other experiment (Kennerly and Bonham

1978). This could not be established unambiguously as we obtained few data points below 1 eV.

In the light of the arguments discussed above, it is clear that the technique of photoelectron spectroscopy used in the present experiment for the measurement of electron-atom scattering cross sections at low electron energies, is at least as good as other techniques (time of flight, swarm, etc) used by other investigators. Work is going on in our laboratory to measure electron scattering cross sections for argon, krypton and xenon. From the preliminary results obtained so far it appears that photoelectron spectroscopy may be a better method for measuring scattering cross sections at low electron energies.

Acknowledgments

The authors would like to thank Dr V B Sheorey for useful discussions during the experiment.

References

Charlton M, Griffith T C, Heyland G R and Twomey T R 1980 *J. Phys. B: At. Mol. Phys.* **13** L239-44
Edmonds T and Hobson J P 1965 *J. Vac. Sci. Technol.* **2** 182-97
Gardner J L and Samson J A R 1973 *J. Electron Spectrosc. Relat. Phenom.* **2** 267-75
Kennerly R E and Bonham R A 1978 *Phys. Rev.* A **17** 1844-54
Kumar V and Krishnakumar E 1981a *J. Electron. Spectrosc. Relat. Phenom.* **22** 109-18
—— 1981b *J. Electron. Spectrosc. Relat. Phenom.* **24** 1-9
McEachran R P and Stauffer A D 1985 *Phys. Lett.* A **107** 397-9
Nesbet R K 1979 *Phys. Rev.* A **20** 58-70
Nickel J C, Imre K, Register D F and Trajmar S 1985 *J. Phys. B: At. Mol. Phys.* **18** 125-33
O'Malley T F and Crompton R W 1980 *J. Phys. B: At. Mol. Phys.* **13** 3451-64
Salop A and Nakano H H 1970 *Phys. Rev.* A **2** 127-31
Samson J A R 1967 *Techniques of Vacuum Ultraviolet Spectroscopy* (New York: Wiley)
Stein T S, Kauppila W E, Pol V, Smart J H and Jesion G 1978 *Phys. Rev.* A **17** 1600-8